Numerical Simulation of Four-Point Bending Test on Steel Fiber-Reinforced Concrete Specimens Using DIANA FEA

Mariane R. Rita[1], Igor A. Fraga[1,2], Ana B. C. G. Silva[1,3], Eduardo M. R. Fairbairn[1], Jose C. F. Telles[1], Alexandre Landesmann[1]

[1]*Civil Engineering Program (PEC/COPPE), Federal University of Rio de Janeiro*
Av. Horacio Macedo, 2030 - Bloco I-116 - Cidade Universitária, Rio de Janeiro, Brazil.
mariane_rita@numats.coc.ufrj.br, ifraga@coc.ufrj.br, anabeatrizgonzaga@coc.ufrj.br, eduardo@coc.ufrj.br
[2]*Building Technical Program, fluminense Federal Istitute of Education, Science and Technology (IFF)*
Av. João Jazbick - Santo Antônio de Pádua - Rio de Janeiro, Brazil
Igor.fraga@iff.edu.br
[3]*Department of Structures, Polytechnic School, Federal University of Rio de Janeiro*
Cidade Universitária, Centro de Tecnologia D205, Zip-Code 21945-970, Rio de Janeiro, Brazil

Abstract. This study presents a numerical investigation of the behavior of steel fiber-reinforced concrete specimens under three-point bending tests employing different model approaches. Steel fiber-reinforced concrete has gained significant attention in the construction industry due to its enhanced mechanical properties, including improved ductility and crack resistance. Understanding its behavior under loading conditions is crucial for optimizing structural design and ensuring durability. The simulations were conducted using DIANA Finite Element Analysis (FEA) software, and the comparative analysis was design to compare their effectiveness in predicting the structural response. The simulations were validated against experimental data from laboratory tests to ensure the accuracy and reliability of the numerical predictions. Through comparative analysis, this study evaluates the performance of each modeling approach in predicting key parameters such as load-displacement response, crack mouth opening and ultimate failure mode. Insights gained from these comparisons will provide valuable guidance for selecting the most appropriate modeling technique for similar structural analyses in practical engineering applications.

Keywords: Steel Fiber-Reinforced Concrete, Three-Point Bending Test, Numerical Simulation, Structural Analysis

1 Introduction

Steel fiber-reinforced concrete (SFRC) represents a significant advancement in the field of construction materials. The incorporation of steel fiber reinforcement enhances the mechanical behavior of the material when subjected to direct tensile and bending loads. This improvement results in increased strain capacity, greater toughness, and improved post-cracking behavior, effectively reducing brittleness (ACI [1], Bentur and Mindess [2]). Consequently, steel fibers can serve as supplementary reinforcement alongside traditional steel bars, particularly in thin plate structures and during structural rehabilitation (Grabois et al. [3]).

Despite its advantages, modeling SFRC presents considerable challenges. The accurate determination of the uniaxial tension constitutive law in the post-cracking phase is notably influenced by factors such as fiber distribution and other material parameters [4]. As a result, achieving a precise representation of SFRC behavior is complex and demands sophisticated analytical approaches.

In this context, the present study focuses on conducting numerical simulations of SFRC specimens subjected to a four-point bending test using the finite element analysis software DIANA FEA. The aim is to explore various modeling approaches to predict the behavior of SFRC specimens under bending loads. By systematically comparing these different approaches, the study seeks to identify the most accurate and efficient method for analyzing SFRC behavior and estimating critical model parameters. This comparison will provide insights into the effectiveness of different modeling strategies and contribute to the advancement of SFRC analysis in practical engineering applications.

2 Numerical Modeling

The numerical modeling of the fiber-reinforced concrete beam is being developed using the commercial software DIANA Finite Element Analysis (FEA), designed for finite element analyses applied to structural, geotechnical, and civil engineering problems. This section will present the methodology employed for the numerical modeling of the composite beam subjected to the four-point bending test.

2.1 Constitutive models for fiber reinforced concrete

In the simulations conducted in this study, concrete behavior is characterized using a constitutive crack model based on total strain, which describes stress as a function of deformation. This model is developed along the lines of the Modified Compression Field Theory, originally proposed by Vecchio and Collins [5], and employs a smeared cracking approach for fracture energy. The three-dimensional extension of this theory was proposed by Selby and Vecchio [6]. When considering total stress-strain relationships, different approaches can be taken. For example, the rotating crack model evaluates stress-strain relationships along the principal directions of the strain vector. In contrast, the fixed crack model assesses stress-strain relationships in a coordinate system that remains unchanged after cracking. In all conducted simulations, the fixed crack model was chosen, as it better represents the physical nature of the cracking concept.

To define the constitutive model it is necessary to establish the governing laws that dictate the material's behavior under tension and compression. Therefore, in order to identify the most accurate representation for steel fiber-reinforced concrete, two distinct models in terms of concrete behavior under tension and compression were used. Since the mechanical property that is significantly influenced by the fibers is the residual post-cracking tensile strength, that represents an important design parameter for FRC structures (di Prisco et al. [7]), the two models chosen to represent the tensile behavior takes into account this phenomenon in two different ways: the first chosen model is based on fracture energy with a linear softening curve, related to a crack bandwidth as is usual in smeared crack models. The second one is not directly related to the fracture energy but describes the tensile failure model for fiber reinforced concrete based on force force versus crack mouth opening. This constitutive models are depicted in Fig. 1.

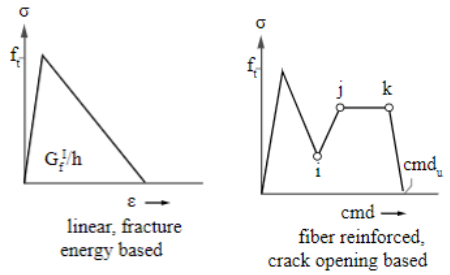

Figure 1. Constitutive models employed to represent the behavior of concrete under tension (DIANA [8]).

To describe the compressive behavior of the SFR concrete the employed constitutive models were Thorenfeldt and Parabolic as shown in Fig. 2. The Thorenfeldt [9] compression curve is described according eq. (1) and eq. (2), through the parameters n, k. Additionally the model has a length scale parameter of Thorenfeldt curve for its post-peak part. Thus, the post-peak horizontal axis scales with the crack bandwidth divided by this scaling parameter.

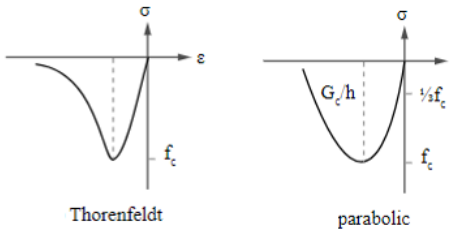

Figure 2. Constitutive models employed to represent the behavior of concrete under compression (DIANA [8]).

$$f = -f_p \frac{\alpha}{\alpha_p} \left(\frac{n}{n - (1 - (\frac{\alpha}{\alpha_p})} \right)^{nk} . \tag{1}$$

$$n = 0.80 + \frac{f_{cc}}{17} \quad ; \quad k = \begin{cases} 1 & ; \quad \text{if } \alpha_p < \alpha < 0 \\ 0.67 + \frac{f_{cc}}{62} & ; \quad \text{if } \alpha \leq \alpha_p \end{cases} \tag{2}$$

The parabolic curve is a formulation based on fracture energy, according to Feenstra [10] and it is described by three characteristic values. The strain $\alpha_c/3$ at which one-third of the maximum compressive strength f_c is reached when $\frac{\alpha_c}{3} = -\frac{1}{3}\frac{f_c}{E}$. The strain α_c at which the maximum compressive strength is reached, is $\alpha_c = -5/3\frac{f_c}{E} = 5\alpha_c$. The values of $\alpha_c/3$ and α_c are determined irrespective of of the element size or compressive fracture energy. The ultimate strain α_u, at which the material is completely softened in compression, is as follows in eq. (3).

$$\alpha_u = \min \left(\alpha_c - \frac{3}{2}\frac{G_c}{h f_c}, 2.5\alpha_c \right) \tag{3}$$

The parabolic compression curve is described according Eq. (4).

$$f = \begin{cases} -f_c \left(\frac{1}{3}\right) \frac{\alpha_j}{\alpha_{c/3}} & ; \quad \text{if} \quad \alpha_{c/3} < \alpha_j \leq 0 \\ -f_c \left(\frac{1}{3}\right) \left(1 + 4 \left(\frac{\alpha_j - \alpha_{c/3}}{\alpha_c - \alpha_{c/3}} \right) - 2 \left(\frac{\alpha_j - \alpha_{c/3}}{\alpha_c - \alpha_{c/3}} \right)^2 \right) & ; \quad \text{if} \quad \alpha_c < \alpha_j \leq \alpha_{c/3} \\ -f_c \left(1 - \left(\frac{\alpha_j - \alpha_c}{\alpha_u - \alpha_c} \right)^2 \right) & ; \quad \text{if} \quad \alpha_u < \alpha_j \leq \alpha_c \\ 0 & ; \quad \text{if} \quad \alpha_j \leq \alpha_u \end{cases} \tag{4}$$

The interaction between both the load and support plates are represented using the linear interface model which defines a linear elasticity behavior for the interface between the steel plates and the concrete. In this model, the parameter that need to be explicitly specified by the user is the linear elastic stiffness for the normal and shear directions.

3 Finite Element Analyzes of the three-point bending test

A two-dimensional numerical simulation of a four-point bending test was conducted on a steel fiber-reinforced concrete beam using the finite element method. The beam's geometry and dimensions are depicted in Fig. 3. The beam features a notch in the transverse direction, with a width of 2.5 mm and a depth of 18 mm. This figure illustrates the finite element mesh, consisting of 6448 elements, along with boundary conditions that mirror the experimental setup.

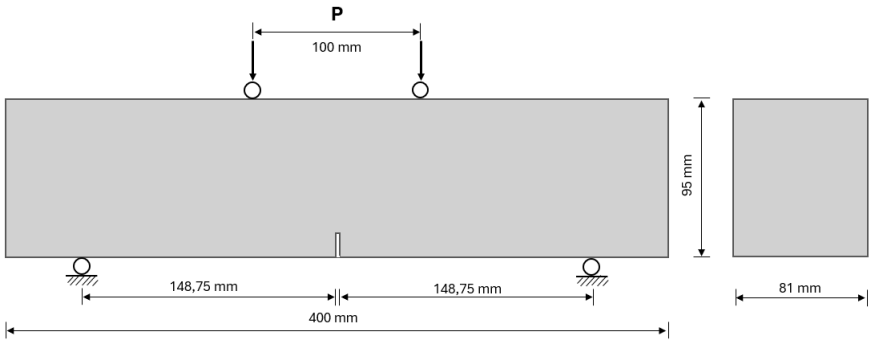

Figure 3. Geometry and dimensions of the notched beam specimen.

The concrete used as the reference in the finite element simulations is a lightweight self-compacting concrete with 0.5% steel fiber inclusion. The primary mechanical properties of this concrete are as follows: mean compressive strength f_c = 30.2 $\times 10^6$ N/m^2; Young's Modulus E_c = 1.9 $\times 10^{10}$ N/m^2; Poisson's ratio $\nu = 0.2$; flexural strength f_{1c} = 3.73 $\times 10^{10}$ N/m^2 and Mode I fracture energy $G_{IC} = 2400$ N/mm, both obtained through four-point bending tests. The Young's Modulus and Poisson rate used for the steel support and load plates are E_{sup} = 210 GPa and ν_{sup} = 0.3, respectively. The parameters of the linear interface between the steel plates and the concrete are as follows: normal stiffness reduction modulus $D_{nn} = 1 \times 10^8$ N/mm^3 and shear stiffness reduction modulus $D_{nn} = 1 \times 10^6$ N/mm^3.

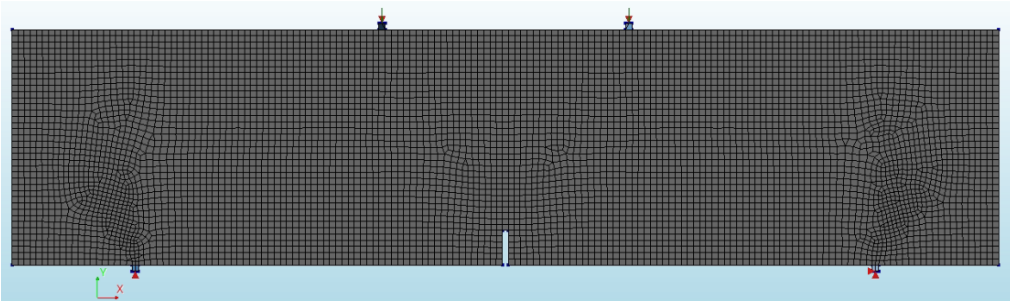

Figure 4. Finite element mesh and boundary conditions.

The finite element analyses investigated the combination of four constitutive models selected to represent the behavior of SFRC under tension and compression. A description of the models used in each simulation is provided in Table 1, and the parameters for each model are detailed in Table 2. Since the chosen crack orientation is fixed, it is necessary to specify the shear retention function, which describes how the shear behaviour changes when the material is cracked. The constant function was chosen with the value $\beta = 1 \times 10^{-6}$.

Table 1. Description of the performed simulations.

Numerical Simulation ID	Tensile model	Compressive model
NS1	Linear, fracture energy based	Thorenfeldt
NS2	Linear, fracture energy based	Parabolic
NS3	Fiber reinforced, crack opening based	Thorenfeldt
NS4	Fiber reinforced, crack opening based	Parabolic

To define the behavior of concrete under tension, considering the effects of steel fiber inclusion, the fracture energy-based model and the fiber reinforced based on crack opening model were chosen. For this, it is necessary to provide values for tensile strength, Mode I fracture energy, and the Force×CMOD (crack mouth opening displacement) points obtained through a three-point bending test. As the available experimental results referred to the four-point bending test, the data used in the model were adjusted, considering that it is known that the three-point test shows slightly higher strength values (di Prisco et al. [7]).

To solve the nonlinear problem, the Newton-Raphson method was utilized. The convergence criteria for force and energy were set at 0.01 and 0.001, respectively. Additionally, line search was employed, and Arc Length control with the Updated Normal Plane method was applied to the vertical displacement of the beam nodes.

3.1 Results and discussions

Fig. 5 illustrates the force-deflection curve derived from the numerical simulations, showcasing comparisons between the various constitutive models. The finite element analysis (FEA) results are satisfactory, revealing differences in the mechanical behavior of the specimen depending on the constitutive models. Additionally, Fig. 6 provides a comparison of the four numerical force-deflection curves. The cracking pattern observed during the four-point bending test is depicted through the crack opening field in the cracked elements shown in Fig. 7. The results, which show crack propagation at the notch, align well with the observed behavior in experimental tests.

Table 2. Model Parameters of tensile and compressive behavior.

Model	Property	Value
Linear, fracture energy based	Tensile strength	$f_t = 1.6 \times 10^6$ N/m^2
	Residual tensile strength	$f_{t,res} = 0.3 \times 10^6$ N/m^2
	Mode I fracture energy	G_{IC} = 900 N/m
Fiber reinforced, crack opening based	Force at onset of crack FL	7630 N
	Force FRi and crack mouth opening at FRi	5320 N; 0.133 mm
	Force FRj and crack mouth opening at FRj	5530 N; 0.26 mm
	Force FRk and crack mouth opening at FRk	4480 N; 2.15 mm
	Ultimate crack mouth opening	3.67 mm
	Crack bandwidth specification	Rots
	Stress factor FRC model	1.12
Thorenfeldt	Compressive strength	$f_c = 30.2 \times 10^6$
	parameter n	2.66
	parameter k	1.5
	length scale parameter	–
	Residual compressive strength	12×10^6 N/m
Parabolic	Compressive strength	$f_c = 30.2 \times 10^6$
	Compressive fracture energy	24000 N/m
	Residual compressive strength	12×10^6 N/m
	Crack bandwidth specification	Rots

As can be observed, in the studied cases, the predominant factor influencing the material's overall behavior is the tensile constitutive model. When the tensile constitutive model is held constant and the compression model is varied, the differences in results are minimal. However, altering the tensile behavior model leads to significantly different outcomes. Simulations NS1 and NS2 exhibit slightly higher peak loads compared to NS3 and NS4, suggesting that the choice of tensile model is critical in capturing the peak load capacity. Furthermore, simulations utilizing the fiber model display characteristics more aligned with the expected results for this type of test, indicating a more accurate representation of SFRC behavior under bending loads.

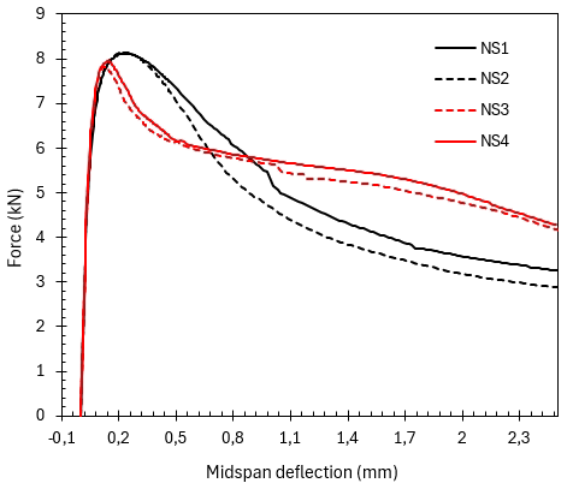

Figure 5. Curve force versus deflection obtained with the used model.

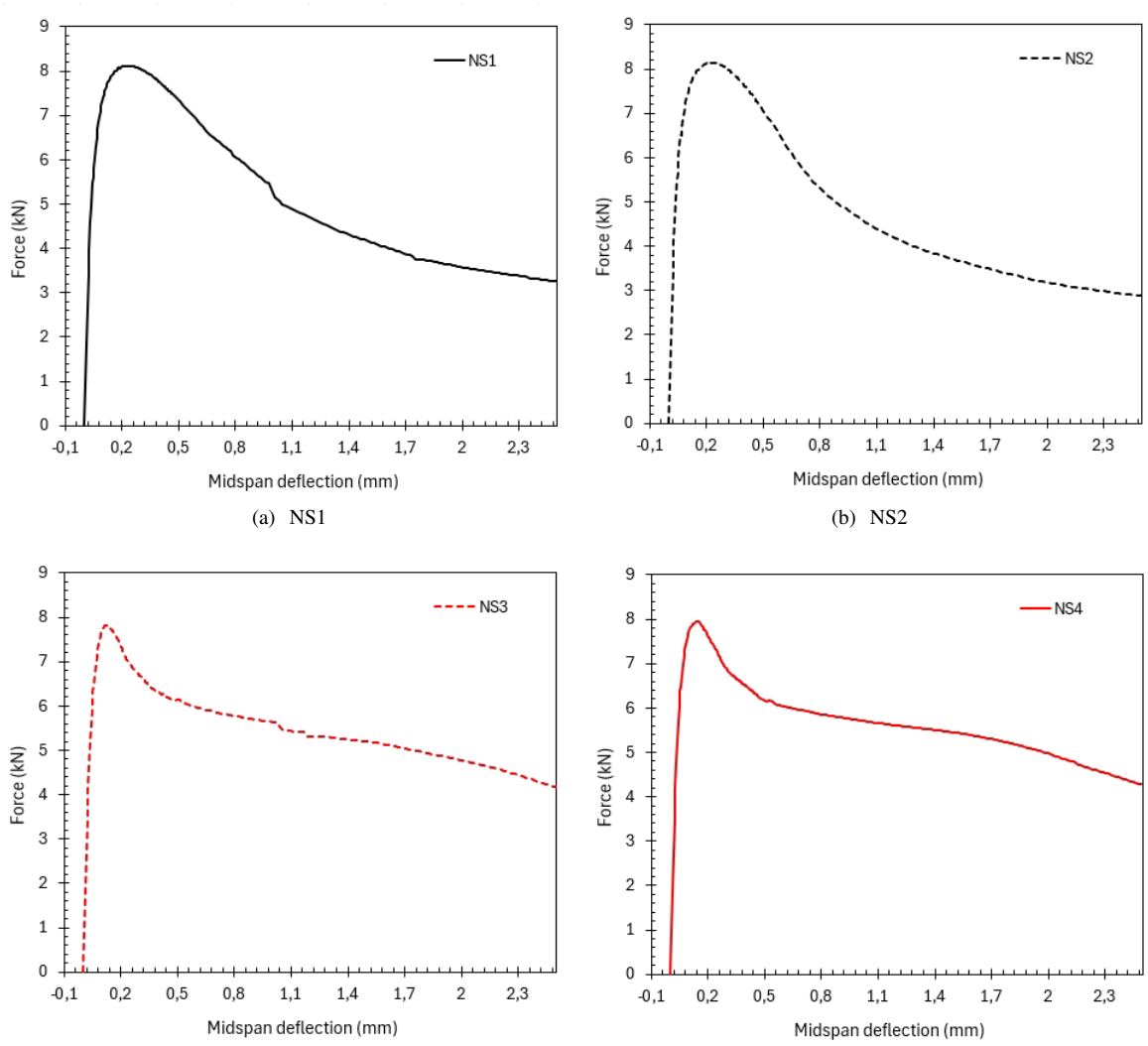

(a) NS1 (b) NS2

(c) NS3 (d) NS4

Figure 6. Comparison of the numerical models simulations with the experimental data.

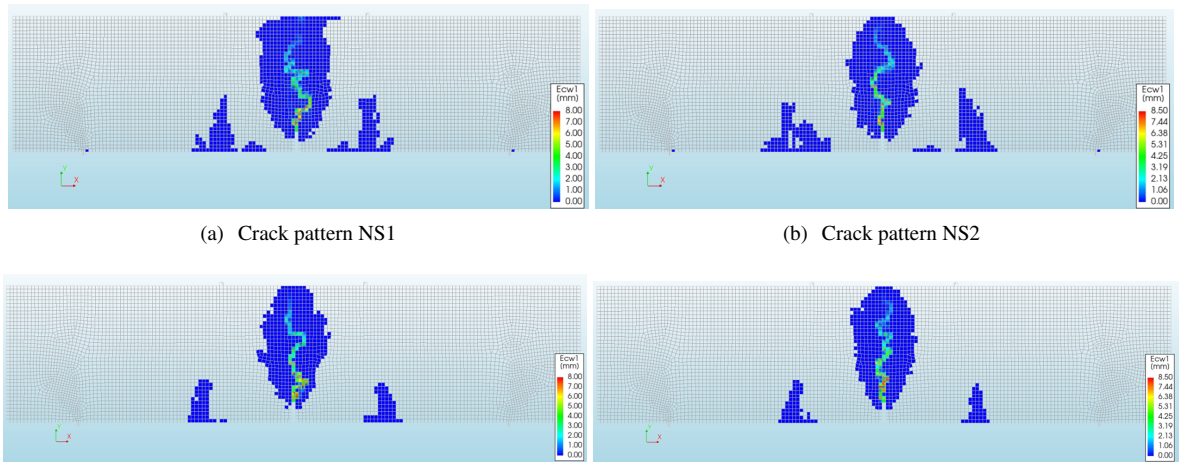

(a) Crack pattern NS1 (b) Crack pattern NS2

(c) Crack pattern NS3 (d) Crack pattern NS4

Figure 7. Comparison of the numerical models simulations with the experimental data.

4 Conclusions

This study presented a comprehensive analysis of steel fiber-reinforced concrete (SFRC) beams subjected to a four-point bending test using finite element method. Four constitutive models were explored to represent both the tensile and compressive behavior of SFRC. The numerical results demonstrated a satisfactory correlation with this kind of experimental test, reproducing adequately the complex post-peak behavior of the material. The finite element simulations conducted in this study not only enhance our understanding of the numerical models and their parameters but also provide a solid foundation for future research. These simulations offer insights into the application of different constitutive models and their effectiveness in analyzing SFRC behavior across various scenarios. Furthermore, the availability of diverse constitutive models is crucial for accurate analysis, as some models may be impractical depending on the data available, potentially leading to results that deviate from real-world behavior and impact safety.

Acknowledgements. The authors are partially supported by the Brazilian funding agencies CNPq and FAPERJ. This study was financed in part by the Coordenação de Aperfeiçoamento de Pessoal de Nível Superior - Brasil (CAPES) - Finance Code 001.

Authorship statement. The authors hereby confirm that they are the sole liable persons responsible for the authorship of this work, and that all material that has been herein included as part of the present paper is either the property (and authorship) of the authors, or has the permission of the owners to be included here.

References

[1] ACI. State-of-the-art report on fiber reinforced concrete. Technical report, (ACI544.1R-96). American Concrete Institute (ACI), 1996 (Reapproved 2002).
[2] A. Bentur and S. Mindess. Concrete beams reinforced with conventional steel bars and steel fibres: properties in static loading. *International Journal of Cement Composites and Lightweight Concrete*, vol. 5, n. 3, pp. 199–202, 1983.
[3] T. M. Grabois, G. C. Cordeiro, and R. D. Toledo Filho. Fresh and hardened-state properties of self-compacting lightweight concrete reinforced with steel fibers. *Construction and Building Materials*, vol. 104, pp. 284–292, 2016.
[4] di M. Prisco, G. Plizzari, and L. Vandewalle. Fibre reinforced concrete: new design perspectives. *Materials and Structures*, vol. 42, pp. 1261–1281, 2009.
[5] F. J. Vecchio and M. P. Collins. The modified compression-field theory for reinforced concrete elements subjected to shear. *ACI Journal 83*, vol. 22, pp. 219–231, 1986.
[6] R. G. Selby and F. J. Vecchio. Three-dimensional constitutive relations for reinforced concrete. Technical report, Tech. Rep. 93-02, Univ. Toronto, dept. Civil. Eng., 1993.
[7] di M. Prisco, M. Colombo, and D. Dozio. Fibre-reinforced concrete in fib model code 2010: principles, models and test validation. *Structural Concrete*, vol. 14, n. 4, pp. 342–361, 2013.
[8] DIANA. *DIANA 10.9 User's Manual*. DIANA FEA bv., Laan van Waalhaven 462, 2497 GR, The Hague, The Netherlands. Available at `https://https://manuals.dianafea.com/d109/?lang=en`, 2024.
[9] E. Thorenfeldt. Mechanical properties of high-strength concrete and applications in design. In *Proc. Symp. Utilization of High-Strength Concrete*, Stavanger, Norway, 1987.
[10] P. H. Feenstra. *Computational aspects of biaxial stress in plain and reinforced concrete*. PhD thesis, Delft University of Technology, 1993.